remote sensing

MDPI

Article

Partitioning Green and Blue Evapotranspiration by Improving Budyko Equation Using Remote Sensing Observations in an Arid/Semi-Arid Inland River Basin in China

Dingwang Zhou [1,2], Chaolei Zheng [1], Li Jia [1,*] and Massimo Menenti [1,3]

[1] Key Laboratory of Remote Sensing and Digital Earth, Aerospace Information Research Institute, Chinese Academy of Sciences, Beijing 100101, China; zhoudw@aircas.ac.cn (D.Z.); zhengcl@aircas.ac.cn (C.Z.); m.menenti@radi.ac.cn (M.M.)
[2] University of Chinese Academy of Sciences, Beijing 100049, China
[3] Faculty of Civil Engineering and Geosciences, Delft University of Technology, 2825 CN Delft, The Netherlands
* Correspondence: jiali@aircas.ac.cn

Abstract: The estimation of water requirements constitutes a critical prerequisite for delineating water scarcity hotspots and mitigating intersectoral competition, particularly in endorheic basins in arid or semi-arid regions where hydrological closure exacerbates resource allocation conflicts. Under conditions of water scarcity, water supplied locally by precipitation and shallow groundwater bodies should be taken into account to estimate the net water requirements to be met with water conveyed from off-site sources. This concept is embodied in the distinction of blue ET (BET) and green ET (GET). In this study, the Budyko hypothesis (BH) method was optimized to partition the total ET into GET and BET during 2001–2018 in the Heihe River Basin. In this region, a better knowledge of net water requirements is even more important due to water allocation policies which reduced water supply to irrigated lands in the last 15 years. This study proposes a modified BH method based on a new vegetation-specific parameter (ω_v) which was optimized for different vegetation types using precipitation and actual ET data obtained from remote sensing observations. The results show that the BH method partitioned GET and BET reasonably well, with a percent bias of 23.8% and 37.4% and a root mean square error of 84.8 mm/a and 113.6 mm/a, respectively, when compared with reported data, which are superior to that of the precipitation deficit and soil water balance methods. A sensitivity experiment showed that the BH method exhibits a low sensitivity to uncertainties of input data. The results documented differences in the contribution of GET and BET to total ET across different land cover types in the Heihe River Basin. As expected, rainfed forest and grassland ecosystems are predominantly governed by GET, with 81.3% and 87.2% of total ET, respectively. In contrast, croplands and shrublands are primarily regulated by BET, with contributions of 61.5% and 84.3% to total ET. The improved BH method developed in this study paves the way for further analyses of the net water requirements in arid and semi-arid regions.

Keywords: water accounting plus; green ET; blue ET; Budyko hypothesis; Heihe River Basin

check for updates

Received: 21 December 2024
Revised: 7 February 2025
Accepted: 7 February 2025
Published: 11 February 2025

Citation: Zhou, D.; Zheng, C.; Jia, L.; Menenti, M. Partitioning Green and Blue Evapotranspiration by Improving Budyko Equation Using Remote Sensing Observations in an Arid/Semi-Arid Inland River Basin in China. *Remote Sens.* **2025**, *17*, 612. https://doi.org/10.3390/rs17040612

Copyright: © 2025 by the authors. Licensee MDPI, Basel, Switzerland. This article is an open access article distributed under the terms and conditions of the Creative Commons Attribution (CC BY) license (https://creativecommons.org/licenses/by/4.0/).

1. Introduction

Water accounting plus (WA+) has been developed as a novel water accounting framework [1,2], which integrates the characteristics of the depletion [3] and the flow methods [4]. WA+ provides spatially comprehensive estimates of water flows, stocks, and consumption

across different land uses, explicitly considering the linkages between water consumption and land use [1,5]. An important feature of WA+ is the separation of the total actual evapotranspiration (ET) into green ET (GET) and blue ET (BET) by considering the sources of water supply. Green water refers to precipitation-derived water stored in the soil, sustaining rainfed ecosystems and agriculture. GET represents the portion of ET sourced only from green water. It is a natural process driven by vegetation use of soil water stored after precipitation events. In contrast, blue water encompasses liquid freshwater resources in surface water bodies (rivers, lakes) and groundwater, typically extracted for human uses such as irrigation. BET quantifies ET supported by an additional water supply through conveyance of blue water, such as irrigation water for croplands or water supplied to ecosystems via canals or groundwater pumping [6,7]. BET reflects human intervention in the water cycle. The distinctions between these components are fundamental. First, green water originates solely from precipitation infiltrating the soil, while blue water is diverted and conveyed from surface or subsurface water bodies. Second, GET is primarily localized, influencing ecosystems and agriculture at regional scales with precipitation patterns and soil conditions dictating water availability. In contrast, BET can have transboundary or global implications, as blue water diversion often involves agricultural systems linked to international water supply chains or depletes shared resources such as transboundary aquifers. This leads to several advantages of the WA+, as demonstrated by existing studies [1,5,8–16]. This includes the following: (i) identification of managed water flows, (ii) quantification of the contributions of different water resource components to water consumption, (iii) better understanding of the interactions between ecosystems and water resources, and (iv) optimization of water use in a catchment.

Although the concept of GET and BET is clear and widely accepted, GET and BET cannot be measured directly. Different algorithms have been developed to partition the total actual ET into BET and GET [17,18]. The precipitation deficit (PD) method, commonly used at annual or longer time scales, directly estimates GET by defining it as the effective precipitation [19,20]. Effective precipitation is the portion of rainfall stored in the soil available for plant transpiration and soil evaporation. BET is estimated as the difference between total actual ET and GET. Another approach to partitioning total actual ET into GET and BET is based on the water balance (WB) method by using a hydrological model [21], in which monthly changes in soil water content in response to precipitation are calculated with a WB model by considering a precipitation-only scenario. Then, GET is assumed to be equal to the negative changes in soil water content. BET is obtained as the difference between independent estimates of total ET (remote sensing data product) and GET. Although these two methods have been widely applied for GET and BET partitioning, they are often criticized for being either low-accuracy or data-intensive and time-consuming. For example, the PD method failed in other regions with abundant precipitation, runoff, and significant fluctuations in groundwater storage [22]. Uncertainties inherent in the hydrological models used in the WB method, particularly regarding parameterizations, assumptions, and more input data in the estimation model, can lead to unreliable ET partitioning results [23].

Simons et al. (2020) [24] demonstrated that the Budyko hypothesis (BH) can be applied to separate GET and BET. The Budyko hypothesis describes the partitioning of long-term precipitation into actual ET and runoff by considering only the dominant controls on actual ET, i.e., water supply (typically precipitation) and energy supply (typically expressed by net radiation) [25]. The method based on the Budyko hypothesis has been used to estimate GET (BET is then calculated by subtracting GET from the total actual ET) in different basins, such as the Lake Urmia in Iran [26], the Kikuletwa catchment in East Africa [27], and other regions. These studies aimed to assess the water consumption patterns, land, or water productivity of irrigated and rainfed agriculture. Compared to the WB method,

the BH method is easier to use since it requires less data and the determination of just one parameter.

While the BH method facilitates broad applicability, its potential relies on selecting an appropriate functional form that captures basin-specific properties. Several analytical functional forms have been proposed for the quantitative description of the Budyko hypothesis. These include the non-parametric original Budyko equation [25], the parametric Fu equation [28,29], and the Mezentsev–Choudhury–Yang equation [30,31]. Compared to the non-parametric Budyko equation, the parametric Budyko equation considers explicitly the influence of land surface properties (i.e., land use and land cover, vegetation characteristics, soil properties, and topographic features) on ET through the basin characteristic parameter, thus enabling the explanation of observed differences relative to the original non-parametric Budyko equation. The Fu equation, derived through dimensional analysis and mathematical reasoning, has been extensively validated across globally diverse catchments, demonstrating reliable and accurate water balance characterization. Therefore, it was adopted in this study for its theoretical robustness and empirical reliability. The parameter (i.e., ω in the Fu equation) represents the integrated effects of basin characteristics and controls the proportion of precipitation consumed as ET, indicating the adjustment of water–energy partitioning related to basin characteristics. Research has shown that the parameter ω in the Fu equation is influenced by various factors, including vegetation factors (such as NDVI, LAI, and vegetation coverage) [32,33], climatic factors (such as climate/precipitation seasonality or coefficient of variation in precipitation) [34,35], soil factors (such as saturated hydraulic conductivity and field capacity) [36–38], topographic factors (such as latitudes, slopes, and elevations) [39–41], and anthropogenic factors (such as irrigated land, cultivated land, urban areas) [40,42]. These factors are closely interconnected and coupled over longtime scales.

Optimizing the value of the parameter ω in the Fu equation is critical to estimate the ratio ET/P. However, the current understanding of how ω controls hydrological partitioning is still very limited. Vegetation integrates the effects of climate, soil, and topography on the water balance and plays an important role in controlling the variability of ω [35]. For example, deep-rooted plants can uptake more water from shallow groundwater reservoirs, thus affecting the response of ET to both precipitation and radiation [43]. Many studies tended to use the default values, or the values applying to large-scale basins. Studies have shown that the parameter ω varies significantly between different sub-basins within the same large basin [33,37,41,44]. Furthermore, studies have shown that significant disparities in ω values can be observed across different regions within the same sub-basin, highlighting the spatial heterogeneity of hydrological processes [45]. This suggests that a single ω parameter may not be able to capture basin, sub-basin, or within-basin characteristics. Therefore, the controls of catchment characteristics on hydrological partitioning vary in different regions of a basin, and the complex (non-linear) interactions between climate and catchment processes result in the spatial heterogeneity of ω. Some studies attempted to construct a universal parameterization model of ω using regression or machine learning methods by selecting primary control factors [32,33,37,41,46–48].

Previous research suggests that aggregating all the vegetation types within a catchment into a single biome may obscure the role of vegetation in determining ω and its spatial variability. Different studies found either positive [49,50] or negative relationships between ω and vegetation characteristics [47]. Therefore, it is necessary to consider the interaction between each vegetation type and climate in determining the partition of precipitation. There are currently no studies on the estimation ω for different ecosystems within a basin. The specific objectives of this study were: (1) to improve the BH method for partitioning GET and BET by estimating a vegetation-specific parameter (ω_v); (2) to evaluate the

performance of the improved BH method; and (3) to analyze the partitioning of total ET into GET and BET across different ecosystems in an arid/semi-arid inland river basin in China.

To obtain better estimates of the parameter (ω_v), we proposed optimizing it using remote sensing data products for precipitation, potential, and actual ET by applying the least squares method. The performance of this approach was evaluated by comparing our estimates with the experimental results at field scale. Additionally, the implications of the GET and BET variability for water management were analyzed.

2. Study Area and Data

2.1. Study Area

The Heihe River Basin (HRB) is the second-largest endorheic river basin in the arid and semi-arid region of northwestern China (37.7°–42.7°N, 97.1°–102.0°E), covering an area of approximately 14.3 × 10^6 ha (Figure 1). The river originates in the Qilian Mountains, which are located on the northern edge of the Tibetan Plateau, and serves as a critical water resource for a large area.

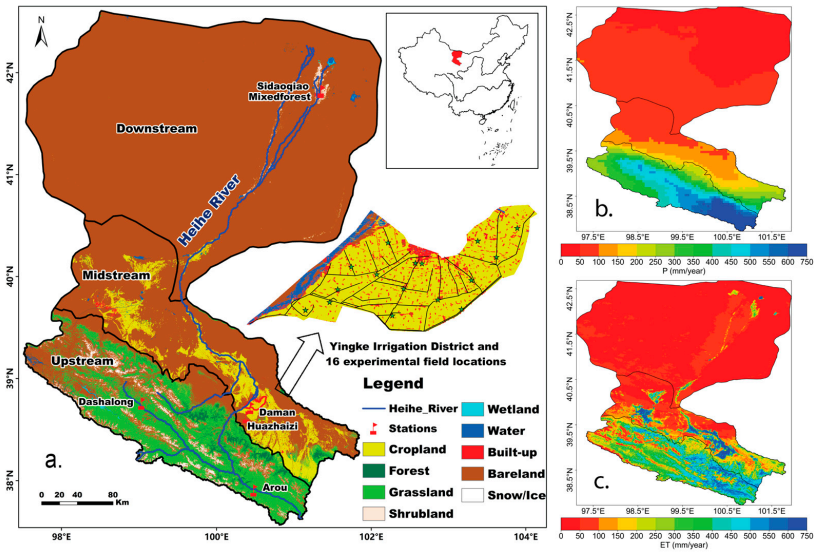

Figure 1. Maps of the Heihe River Basin: (**a**) land use and land cover with the inset map as Yingke Irrigation District (red flags are as the flux tower stations; (**b**) mean precipitation in 2001–2018; (**c**) and mean actual ET in 2001–2018.

The upper reaches, at elevations ranging from 3000 m to 5500 m above sea level (a.s.l.), consist mainly of mountainous terrain with alpine forests and grassland. From 1980 to 2014, the average annual precipitation in the upper reaches was about 500 mm [51].

The middle reaches, at elevations between 1400 m and 1700 m a.s.l., are characterized by extensive agricultural oases. The agricultural oases in this region rely heavily on irrigation to maintain their productivity, using water from the upper reaches of the river as well as groundwater extraction. During the period from 2007 to 2014, the annual precipitation in the middle reaches was around 100–250 mm, while the annual potential ET ranged from 1200 to 1800 mm [52,53].

The downstream region is predominantly barren land or Gobi Desert, with a primary oasis called Ejina dominated by shrubland and some farmland. Scattered natural oases are found along the river and are covered by Populus euphratica, Tamarix, and Haloxylon ammodendron. From 2007 to 2014, the annual precipitation in the lower reaches was less than 50 mm, while the annual potential ET is about 3755 mm [52,53].

2.2. Data and Pre-Processing

2.2.1. Remote Sensing Data

We used remote sensing data products on potential and actual ET, precipitation, and land use land cover at 1 km spatial resolution for the period from 2001 to 2018.

The actual ET data in 2001–2018 were obtained by applying the ETMonitor system [54–56]. The latter estimates global daily actual ET at 1 km spatial resolution (https://doi.org//10.12237/casearth.6253cddc819aec49731a4bc2). Meteorological forcing is extracted from the ERA5 reanalysis dataset. Daily potential ET is estimated using the Penman–Monteith equation with bulk surface resistance equal to zero [57].

Daily precipitation is the Climate Hazards Group Infrared Precipitation with Stations (CHIRPS) data product at 0.05° spatial resolution (https://data.chc.ucsb.edu/products/CHIRPS-2.0/, accessed on 1 December 2024) [58]. The 0.05° CHIRPS precipitation data were downscaled to 1 km resolution using a bilinear interpolation method. While more advanced downscaling methods could be considered in future studies, the bilinear interpolation approach was considered appropriate for the objectives of this study.

Annual land cover data were extracted from the Land Cover Dataset for the Qilian Mountain Area from 2001 to 2018 (V2.0) (https://doi.org/10.11888/Ecolo.tpdc.270916) with a spatial resolution of 30 m (Figure 1a) [59,60]. The International Geosphere–Biosphere Programme (IGBP) classification system was adopted. The 30 m land cover data were upscaled to 1 km spatial resolution using the majority method.

2.2.2. Auxiliary Data

The soil properties from the high-resolution soil map of hydraulic properties (Hi-HydroSoil) with 250 m resolution (https://www.futurewater.eu/projects/hihydrosoil/, accessed on 10 July 2023) [61] were used and upscaled to 1 km resolution to obtain the saturated water content of the plant root zone.

2.2.3. Ground Observations

To assess the accuracy of precipitation and actual ET from satellite observations, we collected in situ latent heat flux data from a total of six flux tower stations in the upper, middle, and lower reaches of the HRB from 2012 to 2021 (Table 1). These stations cover a wide range of land cover, i.e., forest, grassland, cropland, and bare land in the upper to lower reaches of the HRB [62]. Daily ET was obtained from the 30 min latent heat flux measurements by the eddy covariance system, and monthly ET was obtained by accumulating the daily ET values. Data from days with more than 80% missing measurements of 30 min latent heat flux were not used. If in situ flux measurements on more than 25 days in a month were missing, and the monthly data were not used to evaluate the remote sensing actual ET. The 30 min precipitation observed by rain gauges was aggregated to monthly totals.

Table 1. In situ flux tower sites in Heihe River Basin.

Station	Lon (°)	Lat (°)	Elev (m)	Land Cover	Time Period	Location
Arou	100.46	38.05	3033	Grassland	2013–2021	Upstream
Dashalong	98.94	38.84	3739	Grassland	2013–2021	Upstream
Daman	100.37	38.86	1556	Cropland	2013–2021	Midstream
Huazhaizi	100.32	38.77	1731	Bare land	2013–2021	Midstream
Mixedforest	101.13	41.99	874	Forest and Shrubland	2013–2021	Downstream
Sidaoqiao	101.14	42.00	873	Shrubland	2013–2021	Downstream

2.2.4. Literature Data

There were no direct in situ measurements of GET and BET in the HRB to validate our estimates. We used data collected during a field experiment in the Yingke Irrigation District in the middle reaches of the HRB between April and September in 2012–2013 [63,64]. The experiment included 16 fields, covering different soil types and crops in the Yingke Irrigation District (inset map in Figure 1a). Soil water content, soil texture, crop phenology, leaf area index, dry biomass, and plant height were measured. In addition, irrigation time and volume were recorded. Daily meteorological data were collected at the Zhangye weather station (100°25′E, 38°51′N, 1425 m a.s.l.). These field data were used to drive an agro-hydrological model (SIMDualKc model) to estimate GET and BET. Our estimates of BET were evaluated against these observations. The site scale validation was conducted only for BET, since the GET data were not available. Detailed information on the field experiment and methodology can be found in Yan (2015) [63] and Jiang (2017) [64].

3. Methods

3.1. GET and BET Estimation Based on Budyko Hypothesis

The Budyko hypothesis describes the long-term relationships between the water and energy balance in a basin. The hypothesis states that precipitation is the only source of water in closed basins, with some of the precipitation exiting the basin as runoff and some entering the atmosphere via ET [25]. GET, as defined in this study, is given by the partition of precipitation into ET and runoff according to the BH concept (Figure 2).

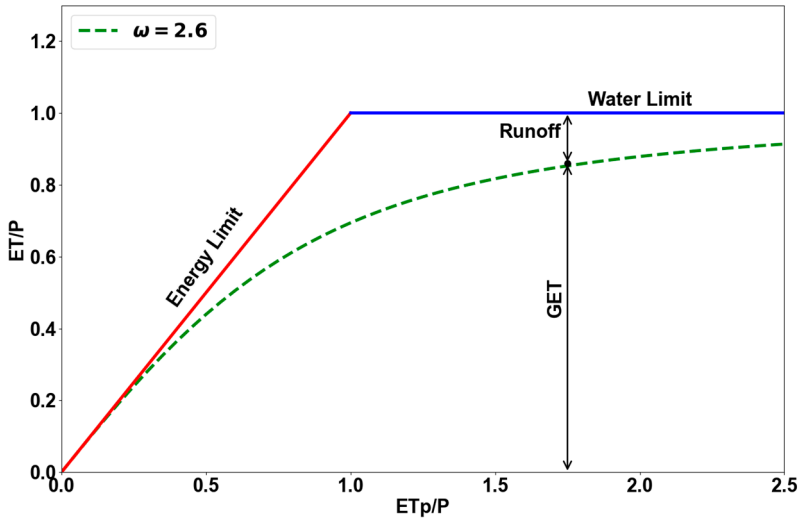

Figure 2. The Budyko curve (dashed green curve) expressed by the Fu equation (ω = 2.6, corresponding to the original Budyko curve). The red line represents the energy limit and the blue line represents the water limit.

The Fu equation [28], derived by dimensional analysis and mathematical deduction, is written as follows:

$$\frac{ET}{P} = 1 + \frac{ET_{\mathrm{p}}}{P} - \left[1 + \left(\frac{ET_{\mathrm{p}}}{P}\right)^{\omega}\right]^{\frac{1}{\omega}} \tag{1}$$

where P is annual precipitation (mm), ET_{p} is annual potential ET (mm), and ω is a basin characteristic parameter in the range (1, +∞) describing the combined effect on actual ET of climatic and basin characteristics. The default ω value is 2.6.

The Fu equation (Equation (1)) assumes that precipitation is the only source of water available for ET in a given catchment and that water storage can be neglected in the water

balance equation on an annual or longer timescale. Simons et al. (2020) [24] applied the Fu equation to estimate GET of a catchment as follows:

$$\frac{GET}{P} = 1 + \frac{ET_{\mathrm{p}}}{P} - \left[1 + \left(\frac{ET_{\mathrm{p}}}{P}\right)^{\omega}\right]^{\frac{1}{\omega}}. \tag{2}$$

The BET is then calculated as the difference between the total actual ET and the GET:

$$BET = ET - GET. \tag{3}$$

To determine GET using Equation (2), the unknowns are precipitation, potential ET, and ω. In principle, ω integrates the effects of basin climate, hydrology, topography, soil, and vegetation. Vegetation integrates the effects of climate, soil, and topography on the water balance and determines the variability of ω. On the one hand, vegetation adapts to the local climate, hydrology, and soil moisture conditions, and on the other hand, it modifies the soil climate and properties to maximize its water use efficiency. This two-way feedback between vegetation, soils, hydrology, and climate is the co-evolutionary process in basins [65]. Thus, each ecosystem has a ω value controlled by vegetation under otherwise similar conditions within a catchment. River basins are typically divided into sub-basins. Assuming that a single vegetation type is dominant in each sub-basin, satisfying the steady-state condition of the Budyko hypothesis, Equation (2) can be written at the annual scale as follows:

$$\frac{GET_{v,i}}{P_{v,i}} = 1 + \frac{ET_{\mathrm{p}v,i}}{P_{v,i}} - \left[1 + \left(\frac{ET_{\mathrm{p}v,i}}{P_{v,i}}\right)^{\omega_v}\right]^{\frac{1}{\omega_v}} \tag{4}$$

where $P_{v,i}$, $ET_{\mathrm{p}v,i}$, and $GET_{v,i}$ are pixel-wise values of annual precipitation, annual potential ET, and annual GET, all with unit mm, in pixel i covered by vegetation type "v", respectively, based on remote sensing data products.

The vegetation-specific parameter ω_v is then estimated by applying the least squares method using Equation (4) to the yearly precipitation and potential ET averages for each year and each vegetation type. The objective function Obj (ω_v) reads then as follows:

$$Obj(\omega_v) = min \sum_{k=Y_0}^{Y_n} \left\{ \frac{ET_{v,k}}{P_{v,k}} - \left\{ 1 + \frac{ET_{\mathrm{p}v,k}}{P_{v,k}} - \left(1 + \left(\frac{ET_{\mathrm{p}v,k}}{P_{v,k}} \right)^{\omega_v} \right)^{\frac{1}{\omega_v}} \right\} \right\}^2 \tag{5}$$

where k is the year number, Y_0 and Y_n represent the start and end year of the analysis, respectively (from 2001 to 2018 in this study); $P_{v,k}$ and $ET_{\mathrm{p}v,k}$ are the annual precipitation and potential ET, respectively, averaged over all pixels covered by vegetation type "v" in year "k" (unit: mm). For a given vegetation type (v) that occupies N pixels, the following equations apply to mean precipitation, potential ET, and actual ET at an annual scale:

$$P_{v,k} = (\sum_{i=1}^{N} P_{v,k}(i))/\mathrm{N} \tag{6}$$

$$ET_{\mathrm{p}v,k} = (\textstyle\sum_{v=1}^{N} ET_{\mathrm{p}v,k}(i))/\mathrm{N} \tag{7}$$

$$ET_{v,k} = (\textstyle\sum_{i=1}^{N} GET_{v,k}(i))/\mathrm{N} \tag{8}$$

There are four dominant vegetation types in the HRB, i.e., forest, grassland, cropland, and shrubland. This fitting is not applicable to irrigated cropland and deep-rooted shrub-

land. Previous studies applied GET values of rainfed croplands to represent neighboring irrigated croplands [18,66]. We applied the rainfed cropland ω_v value to estimate GET and BET in irrigated cropland. Shrubland is primarily distributed in shallow groundwater areas along streams in the extremely arid downstream regions of the HRB, and it relies heavily on groundwater for growth. The shallow groundwater reservoirs are recharged by river water, which strongly depends on irrigation water management [67]. Therefore, Equation (8) is not applicable to shrubland to estimate shrubland-specific values of ω_v. We averaged the forest and grassland ω_v values to estimate the GET and BET of shrubland in the HRB.

3.2. Evaluation Against Alternate Methods

The improved BH method was compared with two commonly used methods to estimate BET and GET. The PD method compares the amount of effective precipitation and actual ET to estimate GET and BET (see Section 3.2.1). Changes in soil water storage can be calculated with the WB method. These changes are then compared with independent estimates of total ET. This comparison allows us to partition ET into BET and GET, as detailed in Section 3.2.2. Both the WB and PD methods were applied at the monthly scale, and the monthly estimates of GET and BET were then accumulated to obtain annual values of GET and BET.

3.2.1. Precipitation Deficit Method (PD)

The precipitation deficit method distinguishes between GET and BET by determining whether the monthly effective precipitation is sufficient to meet the monthly ET demand. Effective precipitation is the fraction of precipitation stored in the soil that can be used for plant transpiration and soil evaporation [68]. When effective precipitation is larger than ET, precipitation can meet water consumption and actual ET is equal to GET. However, when the precipitation is insufficient to meet plant water needs, additional water sources (e.g., surface water or groundwater) are required to meet the water consumption. GET and BET are then calculated as:

$$BET = max(ET - P_e, 0) \tag{9}$$

$$GET = ET - BET \tag{10}$$

where P_e is effective precipitation (mm) that is of great importance for the correct estimation of GET and BET. We applied the same parameterization of P_e as the widely used CROPWAT model [69,70] to estimate the effective precipitation:

$$P_e = \begin{cases} \dfrac{P(125 - 0.2P)}{125}, & P < 250 \\ 125 + 0.1P, & P \geq 250 \end{cases} \tag{11}$$

where P is the total monthly precipitation (mm).

3.2.2. Soil Water Balance Method (WB)

The soil water balance method is based on describing physical processes in each pixel. By tracking the soil moisture balance, with actual ET known a-priori, the method distinguishes between water use that is met solely by precipitation and what requires additional water resources, thereby partitioning actual ET into GET and BET. It calculates the losses of precipitation in the form of surface runoff, vegetation canopy interception, and deep infiltration to obtain the available water (W_t) from precipitation. The GET and BET can be determined by comparing the W_t with the actual ET. If the W_t is larger than the actual ET, the water stored in the soil is sufficient to meet the ET demand. If W_t is less than

the actual ET, the soil water in the soil is insufficient to meet the ET demand, and additional water sources are required. GET and BET are calculated as:

$$GET_t = min(W_t, ET_t) \tag{12}$$

$$BET_t = max(ET_t - GET_t, 0) \tag{13}$$

where t is the monthly time step. W_t is the amount of available water for ET (mm), estimated according to the water balance equation:

$$W_t = SM_{t-1} + P_t - I_t - Q_t - Q_{prec,t} \tag{14}$$

where SM_{t-1} is the soil moisture stored at the end of the previous timestep (mm) and updated at each time step; P_t is precipitation (mm); I_t is the canopy precipitation interception loss (mm) estimated by ETMonitor; Q_t is surface runoff (mm); and $Q_{prec,t}$ is percolation (mm). The detailed calculations for Q_t and $Q_{prec,t}$ can be found in [7,71,72].

3.2.3. Numerical Experiment to Assess the Uncertainty Associated with the Input Data

To evaluate the robustness of the BH method for estimating GET and BET, a numerical experiment was conducted, and the error in partitioning the GET and BET using the satellite-derived dataset (mainly precipitation and ET) was evaluated based on sensitivity analysis. The observed precipitation and ET data were used as a benchmark for the sensitivity analysis and the mean percentage error in remote sensing annual or seasonal ET estimates ranges from 1% to 20%, while the mean percentage error in remote sensing precipitation can typically be up to 65%. Accordingly, we created four scenarios by taking ET equal to plus and minus 20% and 40% of the annual ET observed by the eddy covariance system. Similarly, we created six scenarios for precipitation using plus and minus 20%, 40%, and 80% of the in situ-observed annual precipitation. These error scenarios were plotted to generate a sensitivity curve for further analysis. These curves illustrate the relative errors in the estimated GET and BET resulting from the errors in the input variables (ET and precipitation).

To create a reference dataset, the same numerical experiment was also conducted in the same way for PD and WB methods.

3.2.4. Error Metrics

Percent bias (PBIAS) is a statistical metric used to evaluate the accuracy of estimates:

$$PBIAS = \frac{\sum_{i=1}^{n}(Obs_i - Est_i)}{\sum_{i=1}^{n} Obs_i} \times 100\% \tag{15}$$

where Obs_i is the observed value, Est_i is the estimated value, and n is the number of observations. The optimal value of PBIAS is 0, with positive values indicating overestimation and negative values indicating underestimation.

Root mean square error (RMSE) is quantifying the magnitude of random errors by calculating the square root of the average squared differences between observed values and estimates:

$$RMSE = \sqrt{\frac{1}{n}\sum_{i=1}^{n}(Obs_i - Est_i)^2}. \tag{16}$$

4. Results

4.1. Determination of the Vegetation-Specific Parameter (ω_v) in the BH Method

The ω_v values for each vegetation type in the HRB were determined by fitting satellite-derived annual precipitation, actual ET, and potential ET data from 2001 to 2018 in the HRB (Figure 3). The results show that forest had the highest value ($\omega_{forest} = 9.52 \pm 1.67$) among all the vegetation types. As regards the ratio ET/P, the coefficient of determination (R^2) was 0.53 and RMSE = 0.05. Grassland had a significantly lower value (ω_{grass} = 3.77 ± 0.18), while R^2 = 0.51 and RMSE = 0.04 for the ratio ET/P. This lower value is probably due to the shallower root systems, lower leaf area index (lower vegetation cover), and lower transpiration capacity. This is consistent with previous research showing that higher vegetation cover is associated with both higher ω values and higher evaporation rates. Cropland (rainfed) has a slightly higher value ($\omega_{cropland}$ = 4.99 ± 0.56), while R^2 = 0.43 and RMSE = 0.07 for the ratio ET/P. This higher value may be attributed to management practices such as fertilization and tillage, which likely result in higher ET compared to grassland.

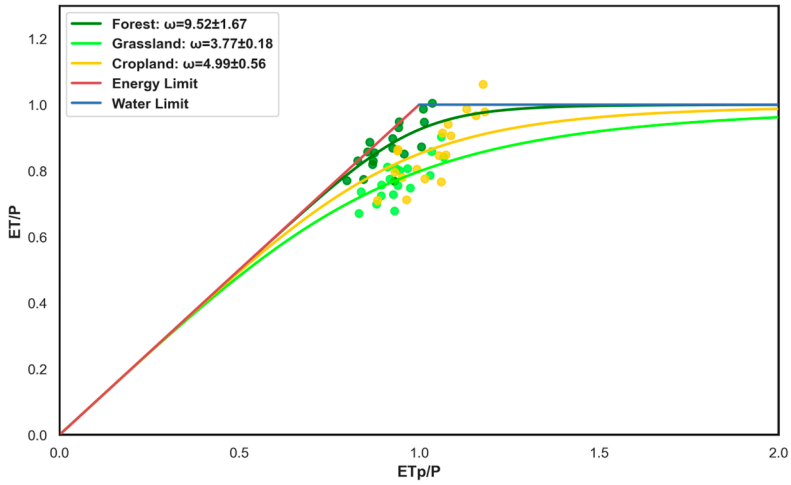

Figure 3. The vegetation-specific model parameter ω_v by fitting satellite-derived precipitation, actual ET, and potential ET in the Heihe River Basin (2001–2018).

4.2. Evaluation of BET and GET Partition

4.2.1. Evaluation at Site Scale

To evaluate the accuracy of the ET partitioning methods, we compared our estimates with the field experiment data described in Section 2.2.4 (Table 2). The BET estimated by the BH method showed good agreement with Yan's results, with PBIAS ranging from 23.8% to 37.4% and root mean square errors (RMSE) ranging from 84.8 mm/a to 113.6 mm/a. In comparison, the WB and PD methods showed slightly larger deviations from the reference data. For the PD method, the deviation is probably due to an underestimation of the effective precipitation using Equation (11). The underestimation of GET leads to an overestimation of BET.

Table 2. Comparison of BET estimates from different methods with experimental results in 16 fields of the Yingke Irrigation District (2012–2013).

Year	Experimental Results (mm/a)	BET (mm/a)			PBIAS (%)			RMSE (mm/a)		
		BH	WB	PD	BH	WB	PD	BH	WB	PD
2012	308.3 ± 90.1	373.8 ± 103.7	381.8 ± 102.0	380.0 ± 103.8	23.8	26.9	25.8	84.8	90.8	89.5
2013	249.4 ± 62.0	346.2 ± 107.1	348.3 ± 106.1	352.9 ± 107.5	37.4	38.3	39.9	113.6	115.0	119.4

4.2.2. Spatial Variability of GET and BET

Evaluating the spatial pattern estimated by different methodologies is helpful for selecting the proper approach to partitioning actual ET into GET and BET. Figure 4 illustrates the spatial distribution of GET and BET from 2001 to 2018 in the HRB using the BH method improved by optimizing the vegetation-specific parameter (ω_v), and the PD and WB methods. A consistent spatial pattern emerges across all methods, with higher GET (lower BET) in the grassland and forest (upper reaches) transitioning to higher BET (lower GET) in the irrigated area (middle reaches) and shrubland (low reaches). The higher GET in the upper reaches implies lower water yield of this sub-basin. This gradient is likely to be a consequence of the combined effects of decreasing precipitation, increasing temperature, and increasing irrigation from upstream to downstream.

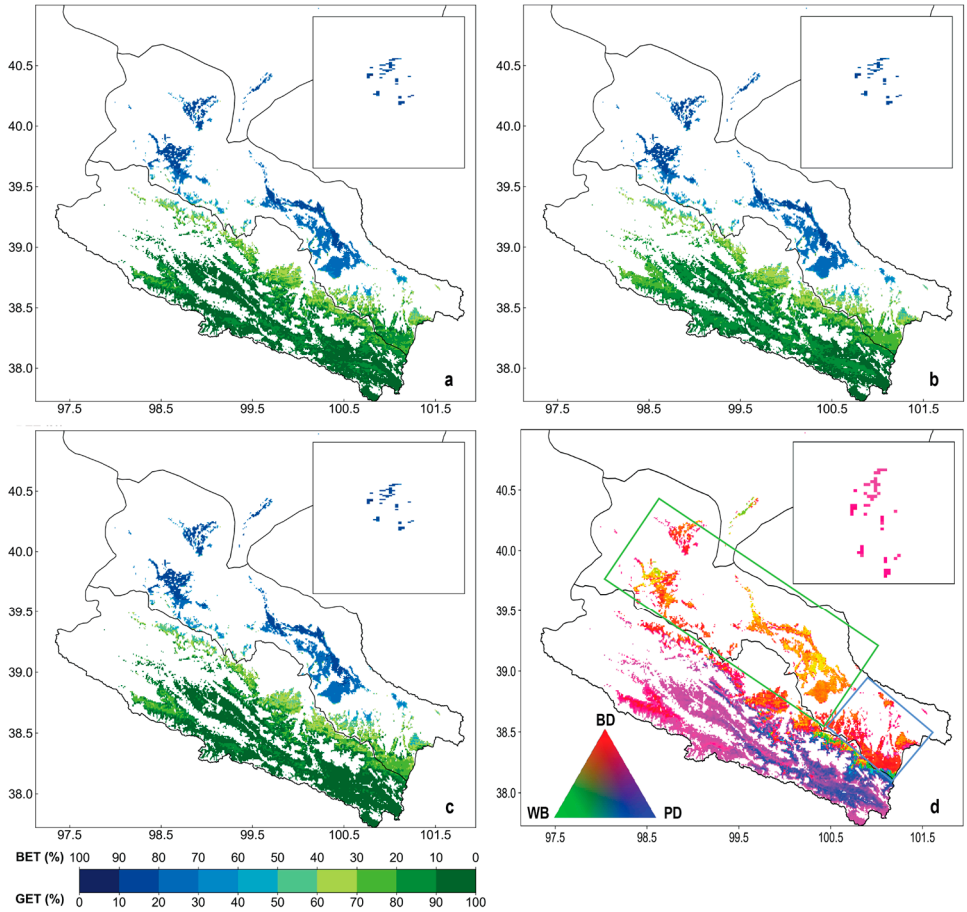

Figure 4. Annual contribution of GET and BET to total ET in the Heihe River Basin (2001–2018) with inset: oasis and shrub contributions, downstream. (**a**) BH method; (**b**) WB method; (**c**) PD method; and (**d**) GET by three methods (red represents BH; green represents WB; and blue represents PD).

While all methods captured the overall pattern, differences were observed (Figure 4d). In the southeastern part of the upper basin, the PD method estimated significantly higher GET (lower BET) than the BH and WB methods. In the northwestern parts of the upper basin, the PD and BH methods produced similar GET estimates, while the WB method produced lower estimates than the other two methods.

In the middle reaches where cropland dominates (Figure 1a), cropland can be classified into two categories based on the contribution of GET and BET to ET (Figure 4a–c). The cropland with a higher fraction of GET (and a lower fraction of BET) is located close to the Qilian Mountains (blue frame in Figure 4d) where precipitation is higher (Figure 1b). The central and western parts (green frame) are characterized by a higher fraction of BET.

The difference in precipitation between the east and the central and western parts may be a possible reason for the differences in BET. Furthermore, the BH method resulted in higher GET values in the blue frame in Figure 4d, while the estimates by the WB and the BH methods were closer in the green frame. Climatic factors (precipitation) are already incorporated in the Budyko framework, and the parameter ω_v has been optimized. The BH method estimates are therefore less affected by uncertainty than the other two methods.

Notably, all the methods gave similar results in the lower reaches and showed the expected lower GET and higher BET. The scarcity of precipitation (Figure 1b) leads to lower GET (higher BET) in downstream areas.

The GET and BET values for the entire basin and its different parts were further analyzed (Table 3). The BH method estimated the highest GET of 317.6 mm/a (with the lowest BET of 128.0 mm/a) for the multi-year average in the whole basin. In the upstream area, the BH method and the PD methods gave GET (BET) approximately 372.0 mm/a (64.8 mm/a), while the WB method gave GET 353.2 mm/a and BET 83.6 mm/a, i.e., different from the other two methods. In the middle reach, the results of the three methods were different. The estimated GET (BET) using the WB and PD methods was approximately 173.8 mm/a (287.3 mm/a). The GET estimate using the BH method was 185.4 mm/a (275.6 mm/a for BET), i.e., slightly different from the estimates obtained using the WB and PD methods. The estimated GET (48.6 mm/a) and BET (244.1 mm/a) in the downstream region were very similar across all three methods.

Table 3. GET and BET values by different methods for the upper, middle, and lower reaches of the Heihe River Basin from 2001 to 2018.

	GET (mm/a)			**BET (mm/a)**		
	BH	**WB**	**PD**	**BH**	**WB**	**PD**
Whole basin	317.6 ± 16.6	301.2 ± 18.3	314.6 ± 17.4	128.0 ± 16.2	144.4 ± 17.1	131.0 ± 15.6
Upstream	372.0 ± 48.7	353.2 ± 48.1	372.8 ± 52.0	64.8 ± 48.3	83.6 ± 46.5	64.0 ± 50.9
Midstream	185.4 ± 33.1	173.8 ± 31.2	174.0 ± 30.3	275.6 ± 24.6	287.3 ± 25.0	287.0 ± 25.1
Downstream	49.8 ± 6.3	48.6 ± 6.0	48.8 ± 6.0	242.5 ± 32.7	244.1 ± 32.1	243.4 ± 32.8

4.3. GET and BET Variability in the Heihe River Basin

Based on the evaluation results in Section 4.2, the improved BH method showed superior performance compared to the other two methods. Therefore, the results of the BH method were used to analyze the BET and GET variability in the HBR.

4.3.1. Temporal Trend of GET and BET in HRB

The trends in GET and BET across the HRB from 2001 to 2018 were estimated using the Mann–Kendall test. The results show significant differences in the trends of GET and BET across the upper, middle, and lower reaches of the basin (Figure 5). In particular, a localized increase in GET was observed in the upper basin (Figure 5c), mirroring the spatial pattern of changes in precipitation (Figure 5a). A significant decrease in BET (Figure 5d) was observed in the western part of the upper basin, corresponding to the localized decrease in ET (Figure 5b) in that area.

In the middle reaches, the BET decreased in the irrigated areas of the west-central part, while it distinctly increased close to the Qilian Mountains in the southeastern part of the basin. The patterns observed for BET are also observed for ET. Figure 5b shows a decreasing trend of ET in the irrigated areas of the west-central part, while an increase is observed close to the Qilian Mountains in the southeastern part. The trend of decreasing BET (5~10 mm/a) in the irrigated area closely follows the decrease in ET, suggesting that reduced ET directly drives the downward trend in BET. This finding is consistent with the

recent water conservation projects implemented in the middle reaches, which resulted in a significant reduction in water consumption per unit area [73,74]. Meanwhile, the increase in BET (2~6 mm/a) close to the Qilian Mountains in the southeastern part mirrors the decrease in precipitation (Figure 5a), implying an increasing demand for blue water (surface water or groundwater) in this region. This pressure is likely to be due to the combined effect of reduced local precipitation and higher air temperature affecting surface water supply in the Heihe agricultural area [75].

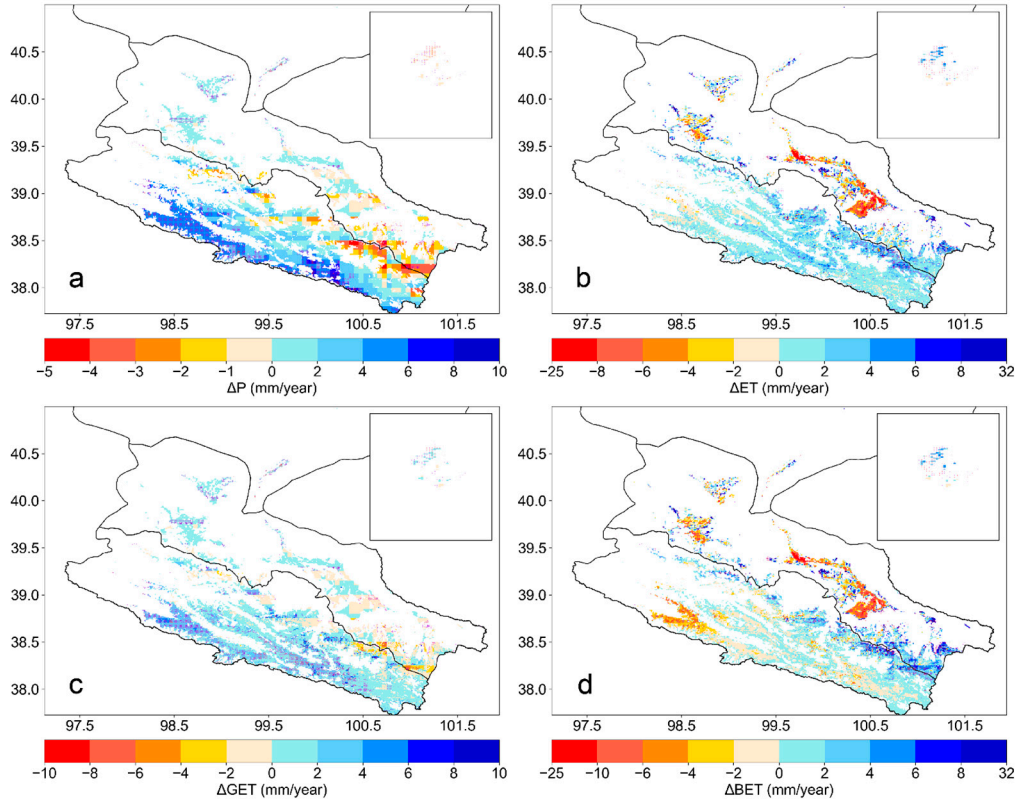

Figure 5. Mean annual deviations from the mean in the spatial distribution of precipitation, ET, GET, and BET in the Heihe River Basin from 2001 to 2018, with insets showing trends in downstream oases and shrubs: (**a**) precipitation; (**b**) ET; (**c**) GET; and (**d**) BET.

In the downstream region, increasing trends in both GET and BET were observed (Figure 5c,d), corresponding to the increase in ET (Figure 5b). However, further analysis is needed to determine whether the increase in ET is due to land use change or the ecological water diversion project aiming at improving water supply to the oases at the northern end of the river.

4.3.2. GET and BET of Different Land Cover Types

Significant differences in GET and BET fractions were observed across different land cover types in the HRB (Figure 6). Forest had the highest total ET and GET, with an exceptionally high GET/ET ratio of 81.3%. This highlights the dependence of forests on green water resources, i.e., precipitation, as its higher GET ratio indicates that almost all the precipitation is used by GET. Grassland also showed a high dependence on green water, with an estimated GET/ET ratio of 87.2%. However, grassland had lower ET than precipitation, resulting in runoff. These significant differences in water consumption patterns highlight the different roles of forests and grasslands in the HRB hydrological cycle: forests act as water-consuming units in the basin hydrological cycle, while grasslands act as runoff-producing units.

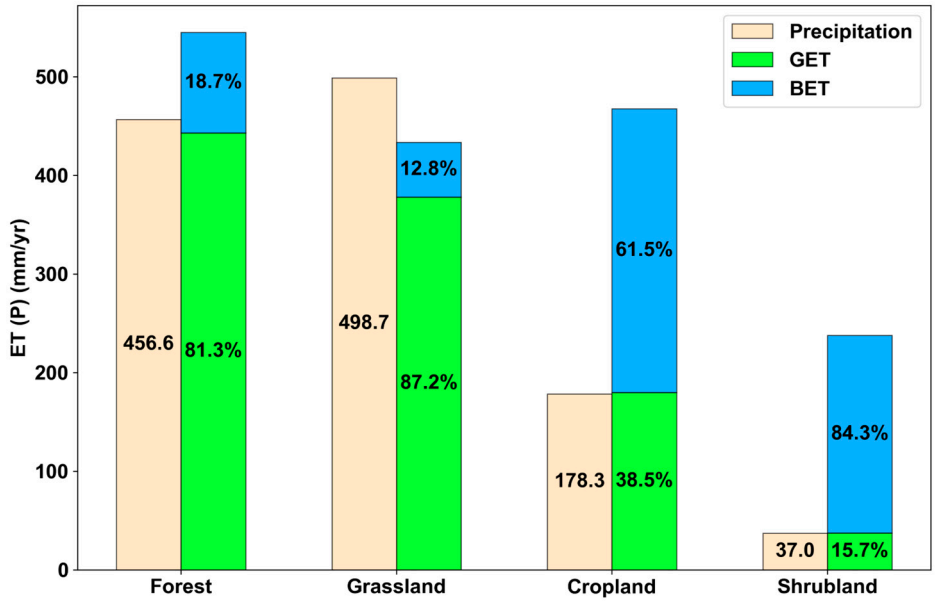

Figure 6. Annual average contributions to ET for different land covers in the Heihe River Basin from 2001 to 2018. The numbers on the precipitation bars are the annual average precipitation; the numbers on the GET (BET) bars are the ratio of GET (BET) to ET; and the height of the GET + BET bars represent the ET.

The cropland in the middle reaches is heavily dependent on irrigation (blue water), which is reflected in the higher BET/ET ratios (61.5%) compared to the vegetation in the upper reaches (i.e., BET/ET for forest and grassland are 18.7% and 12.8%, respectively). Although cropland is the second largest user of water after forest in the HRB (Figure 6), the impact on water resources differs dramatically. Forests in the upper reaches consume large amounts of green water due to higher precipitation and well-developed root systems. In contrast, the high ET of cropland in the middle reaches in a drier climate relies heavily on blue water.

The shrubland, which dominates the downstream region of the HRB with a potential ET of over 2200 mm/a, experiences extreme aridity with minimal precipitation, i.e., not more than 50 mm/a. This large mismatch between precipitation and ET makes the shrubland highly dependent on blue water, not only using all available precipitation, but also extracting six times more blue water (e.g., groundwater) compared to green water (precipitation). The strong dependence of shrubland on blue water resources explains why it grows along the sides of the lower river, where river water supply is largest.

To further explore the distribution of ET sources within each land cover type, we used split violin plots to show the statistics of spatial distribution of GET and BET for each vegetation type (Figure 7). Forest and grassland have a concentrated cluster of GET values in the range of 339.6 mm/a to 485.7 mm/a. In contrast, their BET values differ significantly, with the forest BET showing a wider range and higher peak value compared to the more concentrated and lower peak value of the grassland BET. Crops show a wider range of GET, ranging from 61.0 mm/a to 553.9 mm/a (with a peak around 136.4 mm/a). BET shows two distinct peaks at 110.6 mm/a and 462.4 mm/a. Shrubland has very low GET values, peaking at around 35.7 mm/a, and the BET distribution has a narrow range and a unimodal distribution, peaking at around 226.9 mm/a, indicating the high dependence of these natural land cover types on blue water.

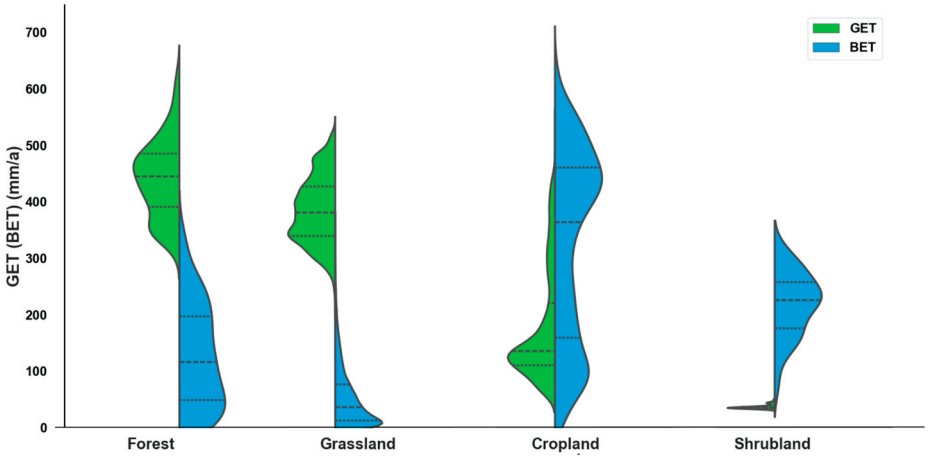

Figure 7. Probability distribution functions of GET and BET for different vegetation covers in the Heihe River Basin from 2001 to 2018 using split violin plots. Interquartile range is shown by short dashes, and median by long dashes.

5. Discussion

5.1. Uncertainty of Estimated GET and BET

5.1.1. Evaluation of P and ET Retrievals

The accuracy of satellite-derived precipitation and ET data, which are crucial inputs for partitioning ET into GET and BET, was evaluated in this study. The evaluation demonstrated a good agreement with the reference data of both the precipitation and ET retrievals. The precipitation reference data were observations at meteorological stations, while the reference ET data were eddy covariance measurements at a few flux towers (Figure 8). The CHIRPS precipitation retrievals at both the upstream (Arou and Dashalong) and the midstream stations (Daman and Huazhaizi) showed a high correlation with the in situ measurements (Figure 8). The bias ranged from 4.08 mm/month to 19.98 mm/month, the RSME ranged from 6.01 mm/month to 32.74 mm/month, and the correlation coefficient ranged from 0.53 to 0.83. The correlation coefficient was lower at the downstream stations compared to the upstream and midstream stations.

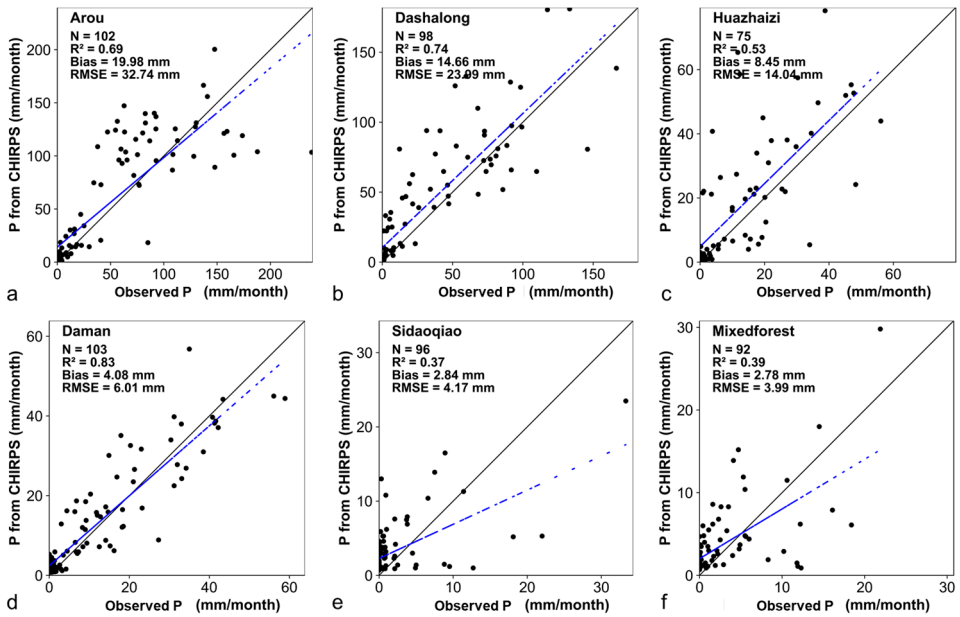

Figure 8. Validation of CHIRPS precipitation data using in situ data in the Heihe River Basin for the period 2013–2021. (**a**,**b**) sites upstream; (**c**,**d**) sites midstream; and (**e**,**f**) sites downstream.

The ETMonitor ET data were evaluated against in situ measurements at the same locations (Figure 9). The ET retrievals for the Arou and Dashalong stations showed a strong correlation with the in situ measurements, with the correlation coefficient values of 0.92 and 0.95, and the RMSE values of 11.3 mm/month and 8.1 mm/month, respectively. Similar results were obtained for the Daman Cropland station, with the correlation coefficient values of 0.91, a bias of 13.36 mm/month, and an RMSE of 17.17 mm/month. Notably, the bias difference was more significant for the downstream Mixedforest station. The difference can be attributed to the heterogeneity of the surroundings of the Mixedforest station, resulting in significant differences between the spatial pattern in the pixel-wise ET retrievals by ETMonitor and the ground observations by the EC system.

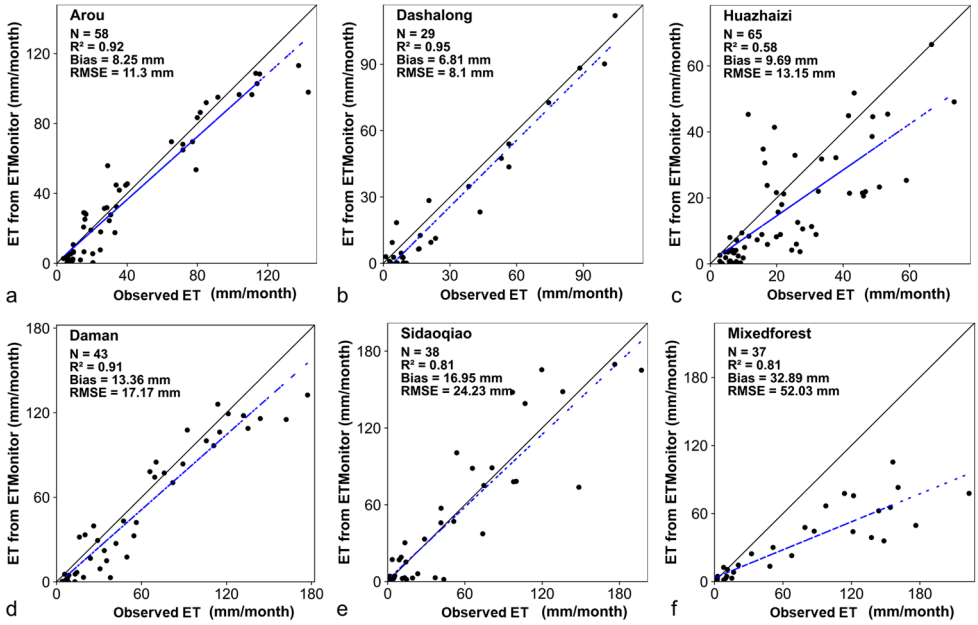

Figure 9. Validation of ETMonitor ET retrievals against EC measurements in 2013–2021 at six sites in the Heihe River Basin. (**a**,**b**) sites upstream; (**c**,**d**) sites midstream; and (**e**,**f**) sites downstream.

Overall, the validation results indicate that the satellite-derived P and ET were reasonably accurate at most stations and could be applied to estimate GET and BET in the HRB.

5.1.2. Uncertainty Propagated from the Input Data

The sensitivity of the BH methods, as well as the PD and WB methods, to P and ET was evaluated as explained in Section 3.2.3. Figure 10 shows that the sensitivity and uncertainty of the GET and BET partitions obtained with different methods are most pronounced in the upstream humid and colder climate zone. The second highest values are observed in the midstream semi-arid climate zone. The downstream arid zone results show low sensitivity and minimal uncertainty in response to changes in precipitation and ET.

In the case of natural vegetation with humid and cold climate, i.e., Arou station with high precipitation and no irrigation, the three methods gave similar results and were all highly sensitive to both precipitation and ET. The ET from ETMonitor was found to be in excellent agreement with the EC measurements at the Arou station (Figure 10b). However, the CHIRPS precipitation data tend to overestimate precipitation compared to the observations at the Arou station, leading to an overestimation of GET and underestimation of BET (Figure 10a).

In a natural ecosystem characterized by an extremely arid climate, i.e., the Sidaoqiao station with very low precipitation and no irrigation, the reliance on ground water is accentuated due to the limited precipitation and absence of irrigation. All three methods gave

similar results and were moderately sensitive to precipitation and ET. CHIRPS precipitation data overestimated precipitation, while the ETMonitor ET data underestimated actual ET (Figure 10e,f). However, despite the large error in precipitation and ET, there was much less uncertainty in the estimated GET and BET, as they were found to be less sensitive to these factors.

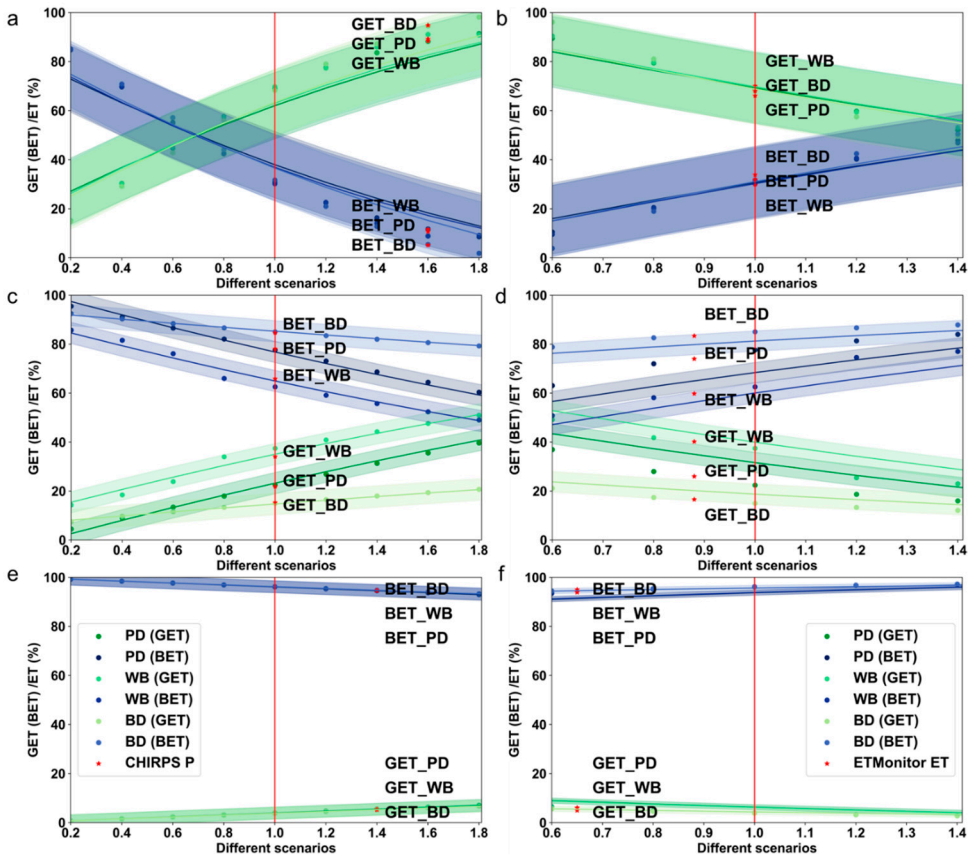

Figure 10. Sensitivity analysis of the different methods to the P and ET in Heihe River Basin. The shaded area depicts the 95% confidence interval. The red line is the benchmark from observed P and ET data. (**a**,**b**) Arou site upstream; (**c**,**d**) Daman site midstream; and (**e**,**f**) Sidaoqiao site downstream.

In Daman station, which represents a transition between humid and arid climate with lower precipitation, irrigation plays a crucial role in ensuring water availability for agriculture. The three methods gave different results, with the BH method showing lower sensitivity to precipitation and ET than the PD and WB methods. This indicates that the error associated with the input precipitation and ET will introduce much less uncertainty in the Daman station. For example, the ETMonitor data at the Daman station underestimated the observed values by approximately 14.05%, resulting in an error of 15.66% in the estimated BET by the BH method. Under the same conditions, the WB and PD methods gave errors of 17.82% and 18.09%, respectively. This highlights the robustness of the BH method, which is much less sensitive to the uncertainty associated with the input data than the PD and WB methods.

5.2. Evaluating Estimates of the ω Parameter in the Budyko Equation

The Budyko hypothesis, in the form of the Fu equation, was used to estimate the GET generated by green water in different ecosystems when the actual ET is known. The estimation of GET using the BH method is significantly influenced by the vegetation-specific parameter ω_v. Previous studies were focused on investigating ω in different basins, while we analyzed ω_v in different ecosystems.

Research has shown that the value of ω varies widely, ranging from 1.0 to infinity. The range in ω_v values in our study is similar to that in the study by Xu et al. (2013) [41], who used a neural network model to estimate ω. They reported values ranging from 1.0 to 4.9 for 224 small basins in the United States, 1.3 to 4.6 for 32 large basins worldwide, and 1.0 to 5.0 for approximately 36,600 basins worldwide. The values of ω_v of our study also compare favorably with Li et al. (2013) [33], who used the same 26 large basins as Xu et al. (2013) [41] and obtained basin-specific ω values ranging from 1.3 to 3.9 by fitting in situ observations (precipitation and ET). The findings of Zhang et al. (2004) [29] were similar to our estimates, i.e., $\omega_{grassland}$ of 3.77 and $\omega_{cropland}$ of 4.99. A large difference was observed for forest, however, as we estimated $\omega_{forest} = 9.52$ against 2.84 in Zhang et al. (2004) [29]. The difference in estimated basin-specific ω values may be attributed to the heterogeneity of vegetation characteristics and their interactions within a basin. This study focuses on the characteristics of different ecosystems in controlling precipitation partitioning to obtain GET, and the values of ω_v in forest ecosystems differ due to these characteristics.

When compared to the outcomes of previous studies, our ω_v values in the HRB exhibited a considerable variability across ecosystems. Figure 11 shows a comparison of ω_v against the basin-scale ω, which is the default value of 2.6, the value (ω = 1.8) estimated by Xu et al. (2013) [41], and the values in six different regions of the HRB by Du et al. (2016) [45]. In particular, Du et al. (2016) [45] used data from observation stations to fit ω values for six different zones in the HRB. Based on the ω values in the original Fu equation fitted by Du et al. (2016) [45], significant differences in ω values were observed even between two climatically similar zones within the HRB, especially in the lower reaches, where ω was 20.28 in one zone and 13.05 in another zone. Furthermore, compared to Du's results, which showed ω values of 1.34 and 1.45 in the upper reaches and 2.05 and 20.28 in the middle reaches, our results differ in the ω_v values between grassland and forest (the dominant vegetation in the upper reaches) and cropland (the dominant vegetation in the middle reaches) (Figure 11).

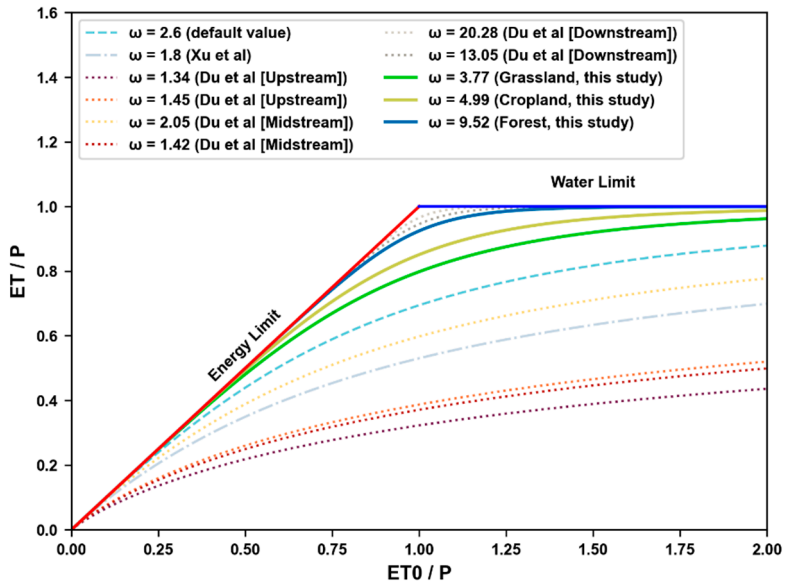

Figure 11. ω_v were compared with results of other studies on the basin's ω [41,45].

Our study confirmed that different ecosystems have different ω_v values even under the same climatic conditions. For example, forest and grassland ecosystems in the cold and semi-arid upper reaches showed differences in ω_v. The significant difference in the values of ω can potentially lead to a greater error in the estimated GET fraction.

5.3. Comparative Assessment of Different Methods

The parametric BH method incorporates the effects of vegetation, soil type, topography, and climate seasonality on ET through a comprehensive parameter ω_v [29,46,47]. We investigated the performance of the BH method in the HRB by calibrating its ω_v value and comparing its estimates with the observed data and those obtained by the WB and PD methods. The results show the superior performance of the BH method in terms of both accuracy and robustness. Compared to the other methods, the estimates by the BH method showed a better agreement with the observed values and lower sensitivity to variations in the input data. The superior performance of the BH method can be attributed to its holistic consideration of multiple influencing factors through the ω_v parameter. This holistic approach makes the BH method more accurate and robust to estimate GET, which is particularly well suited for comprehensive assessments of hydrological dynamics in complex basins such as the HRB, where different climates and ecosystems interact. However, the current applicability of the BH method is limited to annual scales. Attempts have been made to adapt the Budyko framework to monthly estimates [76]. Future research can focus on extending the BH method to higher temporal resolution calculations, improving the accuracy of the ω_v value.

The WB method, based on the water balance principle, includes numerous parameters and relies on empirical formulae to calculate water balance components. Compared to observations and the BH method, WB calculations show larger biases and distinct discrepancies with observations. In particular, lower GET and higher BET are estimated, which implies that a smaller fraction of ET is due to precipitation in ecosystems such as grasslands and forests, which is inconsistent with the findings of previous studies [77,78]. This discrepancy may be due to the inherent underestimation of available water caused by the combination of numerous parameters and empirical formulae used to calculate the water balance components (Equation (14)). Despite these limitations, the WB method has the potential to improve accuracy and can be applied at monthly or even shorter timescales [79]. By addressing the component calculation and parameter calibration, the WB method offers promising prospects for improving its accuracy and achieving finer temporal and spatial resolutions.

The PD method has been widely used due to its clear physical interpretation and applicability to long timescales [1,20,65]. However, evaluations using observational data and sensitivity experiments reveal limitations in its accuracy and high sensitivity to input data. The main source of error comes from the simplified estimation of effective precipitation, which significantly influences the ET partitioning results. The PD method's limited consideration of factors such as plant types, soil properties, precipitation variability, and topography in the calculation of effective precipitation hinders its accuracy [68], particularly in ecosystems where these factors strongly influence water partitioning. Interestingly, although the PD method showed a larger deviation compared to field experiments, it closely matched other methods in the downstream region with an extremely dry climate. This suggests that the method may be more appropriate for arid regions. In wetter areas, such as the upper reaches of the HRB, the high precipitation could mask potential mismatches between precipitation and vegetation water demand, potentially leading to undetected BET.

Overall, the BH method stands out as an ET estimation method with high accuracy, strong robustness, and low sensitivity to input data. Its concise parameterization, clear physical interpretation, and suitability for annual ET assessments make it a valuable tool. The WB method shows promise for improvement, particularly in its accuracy and ability to achieve finer temporal and spatial resolutions. Future research could explore

alternative computational methods, such as machine learning [80,81]. The PD method is a straightforward approach, although its limitations in accuracy require further improvement.

5.4. Advantages of the Research Methods and Applicability in Other Study Areas

This study addresses the critical challenge of partitioning total ET into GET (sourced from precipitation) and BET (sourced from irrigation or groundwater) in arid/semi-arid regions. By optimizing the BH method with ω_v using remote sensing hydrological data, the research provides a robust framework for quantifying and understanding water consumption patterns across ecosystems. This is particularly important in closed basins such as the HRB, where water scarcity and intersectoral competition are exacerbated by limited water availability. The study also highlights the distinct roles of ecosystems (e.g., forests relying on GET vs. croplands depending on BET), offering useful insights for sustainable water management in water-stressed regions.

The Budyko framework explicitly links water–energy partitioning to climatic and vegetation factors, providing a transparent basis for ET partitioning. The modified BH method, by optimizing ωv for different vegetation types (e.g., forest, grassland, and cropland), takes into account ecosystem-specific characteristics. This improves accuracy compared to traditional "one-size-fits-all" approaches. The method relies primarily on globally available remote sensing data (precipitation, ET, and land cover), reducing the dependence on ground-based measurements. The sensitivity analyses (Section 5.1.2) demonstrated that the BH method is less affected by errors in precipitation and ET data compared to the PD and WB methods.

Designed for universal application, the method relies solely on publicly available remote sensing data products, including precipitation, potential, and actual ET. By leveraging open-access remote sensing products, the approach bypasses the need for extensive ground observations, making it viable in regions with limited hydrological monitoring infrastructure. Moreover, by using open-access remote sensing products, our approach can be easily applied to similar inland river basins facing water scarcity, such as those in Central Asia, the Middle East, or Africa, where irrigation-dependent agriculture competes with natural ecosystems. The approach is applicable to any river basin where interannual changes in water storage are negligible when compared with precipitation, ET, and runoff. The proposed vegetation-specific parameter allows adaptation to different land covers (e.g., forests, shrublands, and croplands) and climatic gradients. The method supports water accounting frameworks (e.g., water accounting plus) to evaluate trade-offs between agricultural productivity and ecosystem health, thus informing transboundary water management.

Integrating machine learning or advanced downscaling techniques could further refine parameter optimization and spatial resolution. Overall, this research provides a scalable and adaptable tool for improving water management in global arid/semi-arid zones.

6. Conclusions

The accurate partitioning of ET into GET and BET is crucial for effective water management. Despite its importance, a systematic evaluation and comparison of methods for quantifying GET and BET is lacking in the literature. This study addresses this gap by comparing the performance of an optimized BH method against other established methods for separating ET into GET and BET in the complex climatic and environmental setting of the HRB.

The comparison with observations, numerical experiments, and different methods revealed that the BH method outperformed both the PD and WB methods. The optimized BH method gave the lowest PBIAS (23.8% and 37.4%) and RMSEs (84.8 mm/a and

113.6 mm/a) values for the GET and BET estimates. The BH method had lower sensitivity to uncertainties in precipitation and ET input data. When subjected to a 14.05% uncertainty in ET data, a 15.66% error in its BET estimates was obtained.

Building upon this robust method, this study revealed distinct spatial patterns in GET and BET across the HRB from 2001 to 2018. The upper reaches experienced notably higher GET. Conversely, the middle reaches saw lower BET, likely influenced by water-saving projects focused on, e.g., irrigation efficiency. In the lower reaches, a unique pattern emerged with increases in both GET and BET, potentially resulting from water re-allocation. Furthermore, the study revealed significant differences in water use strategies across vegetation types. Forests and grasslands primarily relied on green water, with GET accounting for 81.3% and 87.2% of their total ET, respectively. This highlights their efficient utilization of local rainfall. In contrast, croplands and shrublands predominantly utilized blue water, with BET contributing to 61.5% and 84.3% of their ET, respectively.

Water resources in the HRB, as in other river basins in arid and semi-arid regions, are limited, and water use for irrigation is being reduced through diverse water management policies. In the HRB, new policies were introduced in the last 15 years to limit water allocation to irrigated lands, so that water supply is lower than both reference and potential ET. Thus, BET became a much more relevant benchmark to assess whether allocation of irrigation water is sufficient to meet net water requirements.

Author Contributions: Conceptualization, D.Z., C.Z., L.J. and M.M.; methodology, D.Z., C.Z., L.J. and M.M.; software, D.Z.; validation, D.Z.; formal analysis, D.Z.; investigation, D.Z., C.Z., M.M. and L.J.; resources, L.J., D.Z. and C.Z.; data curation, D.Z.; writing—original draft preparation, D.Z.; writing—review and editing, D.Z., C.Z., L.J. and M.M.; visualization, D.Z., C.Z., L.J. and M.M.; supervision, L.J., C.Z. and M.M.; project administration, L.J.; funding acquisition, L.J. All authors have read and agreed to the published version of the manuscript.

Funding: This research was funded by the National Natural Science Foundation of China (NSFC) [Grant Nos. 42090014, 42171039]; the Chinese Academy of Sciences President's International Fellowship Initiative [Grant Nos. 2020VTA0001, 2025PVA0200]; and the MOST High Level Foreign Expert program [Grant No. G2022055010L].

Conflicts of Interest: The authors declare no conflicts of interest.

References

1. Karimi, P.; Bastiaanssen, W.G.M.; Molden, D. Water Accounting Plus (WA+)—A Water Accounting Procedure for Complex River Basins Based on Satellite Measurements. *Hydrol. Earth Syst. Sci.* **2013**, *17*, 2459–2472. [CrossRef]
2. Karimi, P.; Bastiaanssen, W.G.M.; Molden, D.; Cheema, M.J.M. Basin-Wide Water Accounting Based on Remote Sensing Data: An Application for the Indus Basin. *Hydrol. Earth Syst. Sci.* **2013**, *17*, 2473–2486. [CrossRef]
3. Molden, D. *Accounting for Water Use and Productivity, SWIM Paper 1*; International Irrigation Management Institute: Colombo, Sri Lanka, 1997.
4. United Nations Statistics Division. *System of Environmental Economic Accounting for Water*; United Nations: New York, NY, USA, 2012; ISBN 978-92-1-161554-8.
5. Dembélé, M.; Salvadore, E.; Zwart, S.; Ceperley, N.; Mariéthoz, G.; Schaefli, B. Water Accounting under Climate Change in the Transboundary Volta River Basin with a Spatially Calibrated Hydrological Model. *J. Hydrol.* **2023**, *626*, 130092. [CrossRef]
6. Falkenmark, M. Land-Water Linkages: A Synopsis. In *FAO, Land and Water Integration and River Basin Management, Proceedings of the FAO Informal Workshop, Rome, Italy, 31 January–2 February 1993*; FAO Land and Water Bulletin 1; Food and Agriculture Organization: Rome, Italy, 1995; pp. 15–16.
7. FAO. *IHE Delft Water Accounting in the Awash River Basin*; FAO WaPOR Water Accounting Reports; Food and Agriculture Organization: Rome, Italy, 2020.
8. Patle, P.; Singh, P.K.; Ahmad, I.; Matsuno, Y.; Leh, M.; Ghosh, S. Spatio-Temporal Estimation of Green and Blue Water Consumptions and Water and Land Productivity Using Satellite Remote Sensing Datasets and WA+ Framework: A Case Study of the Mahi Basin, India. *Agric. Water Manag.* **2023**, *277*, 108097. [CrossRef]

9. Falkenmark, M. Growing Water Scarcity in Agriculture: Future Challenge to Global Water Security. *Philos. Trans. R. Soc. A Math. Phys. Eng. Sci.* **2013**, *371*, 20120410. [CrossRef] [PubMed]
10. Godfrey, J.M.; Chalmers, K. (Eds.) *Water Accounting: International Approaches to Policy and Decision-Making*; Edward Elgar: Cheltenham, Australia, 2012; ISBN 978-1-84980-749-4.
11. Jeyrani, F.; Morid, S.; Srinivasan, R. Assessing Basin Blue–Green Available Water Components under Different Management and Climate Scenarios Using SWAT. *Agric. Water Manag.* **2021**, *256*, 107074. [CrossRef]
12. Kivi, Z.R.; Javadi, S.; Karimi, N.; Shahdany, S.M.H.; Moghaddam, H.K. Performance Evaluation and Verification of Groundwater Balance Using WA+ as a New Water Accounting System. *Environ. Monit. Assess.* **2022**, *194*, 580. [CrossRef] [PubMed]
13. Orth, R.; Destouni, G. Drought Reduces Blue-Water Fluxes More Strongly than Green-Water Fluxes in Europe. *Nat. Commun.* **2018**, *9*, 3602. [CrossRef]
14. Rockstrom, J. *Balancing Water for Humans and Nature: The New Approach in Ecohydrology*; Routledge: London, UK, 2004; ISBN 978-1-84977-052-1.
15. Rockström, J.; Falkenmark, M.; Karlberg, L.; Hoff, H.; Rost, S.; Gerten, D. Future Water Availability for Global Food Production: The Potential of Green Water for Increasing Resilience to Global Change. *Water Resour. Res.* **2009**, *45*, W00A12. [CrossRef]
16. Schyns, J.F.; Hoekstra, A.Y.; Booij, M.J.; Hogeboom, R.J.; Mekonnen, M.M. Limits to the World's Green Water Resources for Food, Feed, Fiber, Timber, and Bioenergy. *Proc. Natl. Acad. Sci. USA* **2019**, *116*, 4893–4898. [CrossRef]
17. Chukalla, A.D.; Krol, M.S.; Hoekstra, A.Y. Green and Blue Water Footprint Reduction in Irrigated Agriculture: Effect of Irrigation Techniques, Irrigation Strategies and Mulching. *Hydrol. Earth Syst. Sci.* **2015**, *19*, 4877–4891. [CrossRef]
18. Msigwa, A.; Chawanda, C.J.; Komakech, H.C.; Nkwasa, A.; van Griensven, A. Representation of Seasonal Land Use Dynamics in SWAT+ for Improved Assessment of Blue and Green Water Consumption. *Hydrol. Earth Syst. Sci.* **2022**, *26*, 4447–4468. [CrossRef]
19. Döll, P.; Siebert, S. Global Modeling of Irrigation Water Requirements. *Water Resour. Res.* **2002**, *38*, 8-1–8-10. [CrossRef]
20. Elbeltagi, A.; Aslam, M.R.; Mokhtar, A.; Deb, P.; Abubakar, G.A.; Kushwaha, N.L.; Venancio, L.P.; Malik, A.; Kumar, N.; Deng, J. Spatial and Temporal Variability Analysis of Green and Blue Evapotranspiration of Wheat in the Egyptian Nile Delta from 1997 to 2017. *J. Hydrol.* **2021**, *594*, 125662. [CrossRef]
21. Karimi, P.; Pareeth, S.; Michailovsky, C. *Rapid Assessment of the Water Accounts in Urmia Lake Basin*; IHE Delft: Delft, The Netherlands, 2019.
22. Senay, G.B.; Friedrichs, M.; Singh, R.K.; Velpuri, N.M. Evaluating Landsat 8 Evapotranspiration for Water Use Mapping in the Colorado River Basin. *Remote Sens. Environ.* **2016**, *185*, 171–185. [CrossRef]
23. Hoekstra, A.Y. Green-Blue Water Accounting in a Soil Water Balance. *Adv. Water Resour.* **2019**, *129*, 112–117. [CrossRef]
24. Simons, G.W.H.; Bastiaanssen, W.G.M.; Cheema, M.J.M.; Ahmad, B.; Immerzeel, W.W. A Novel Method to Quantify Consumed Fractions and Non-Consumptive Use of Irrigation Water: Application to the Indus Basin Irrigation System of Pakistan. *Agric. Water Manag.* **2020**, *236*, 106174. [CrossRef]
25. Budyko, M.I. *Climate and Life*; Academic Press: New York, NY, USA, 1974.
26. Msigwa, A.; Komakech, H.C.; Salvadore, E.; Seyoum, S.; Mul, M.L.; van Griensven, A. Comparison of Blue and Green Water Fluxes for Different Land Use Classes in a Semi-Arid Cultivated Catchment Using Remote Sensing. *J. Hydrol. Reg. Stud.* **2021**, *36*, 100860. [CrossRef]
27. Ghorbanpour, A.K.; Afshar, A.; Hessels, T.; Duan, Z. Water and Productivity Accounting Using WA+ Framework for Sustainable Water Resources Management: Case Study of Northwestern Iran. *Phys. Chem. Earth Parts A/B/C* **2022**, *128*, 103245. [CrossRef]
28. Fu, B. On the Calculation of the Evaporation from Land Surface. *Chin. J. Atmos. Sci.* **1981**, *5*, 23–31. [CrossRef]
29. Zhang, L.; Hickel, K.; Dawes, W.R.; Chiew, F.H.S.; Western, A.W.; Briggs, P.R. A Rational Function Approach for Estimating Mean Annual Evapotranspiration. *Water Resour. Res.* **2004**, *40*, W02502. [CrossRef]
30. Choudhury, B.J. Evaluation of an Empirical Equation for Annual Evaporation Using Field Observations and Results from a Biophysical Model. *J. Hydrol.* **1999**, *216*, 99–110. [CrossRef]
31. Yang, H.; Yang, D.; Lei, Z.; Sun, F. New Analytical Derivation of the Mean Annual Water-Energy Balance Equation. *Water Resour. Res.* **2008**, *44*, W03410. [CrossRef]
32. Cheng, S.; Cheng, L.; Qin, S.; Zhang, L.; Liu, P.; Liu, L.; Xu, Z.; Wang, Q. Improved Understanding of How Catchment Properties Control Hydrological Partitioning Through Machine Learning. *Water Resour. Res.* **2022**, *58*, e2021WR031412. [CrossRef]
33. Li, D.; Pan, M.; Cong, Z.; Zhang, L.; Wood, E. Vegetation Control on Water and Energy Balance within the Budyko Framework. *Water Resour. Res.* **2013**, *49*, 969–976. [CrossRef]
34. Chen, Z.; Wang, W.; Woods, R.A.; Shao, Q. Hydrological Effects of Change in Vegetation Components across Global Catchments. *J. Hydrol.* **2021**, *595*, 125775. [CrossRef]
35. Liu, M.; Lin, K.; Cai, X. Climate and Vegetation Seasonality Play Comparable Roles in Water Partitioning within the Budyko Framework. *J. Hydrol.* **2022**, *605*, 127373. [CrossRef]
36. Abatzoglou, J.T.; Ficklin, D.L. Climatic and Physiographic Controls of Spatial Variability in Surface Water Balance over the Contiguous United States Using the Budyko Relationship. *Water Resour. Res.* **2017**, *53*, 7630–7643. [CrossRef]

37. Bai, P.; Liu, X.; Zhang, D.; Liu, C. Estimation of the Budyko Model Parameter for Small Basins in China. *Hydrol. Process.* **2020**, *34*, 125–138. [CrossRef]
38. Liu, J.; You, Y. The Roles of Catchment Characteristics in Precipitation Partitioning Within the Budyko Framework. *J. Geophys. Res. Atmos.* **2021**, *126*, e2021JD035168. [CrossRef]
39. Koppa, A.; Alam, S.; Miralles, D.G.; Gebremichael, M. Budyko-Based Long-Term Water and Energy Balance Closure in Global Watersheds from Earth Observations. *Water Resour. Res.* **2021**, *57*, e2020WR028658. [CrossRef]
40. Li, Z.; Quiring, S.M. Investigating Spatial Heterogeneity of the Controls of Surface Water Balance in the Contiguous United States by Considering Anthropogenic Factors. *J. Hydrol.* **2021**, *601*, 126621. [CrossRef]
41. Xu, X.; Liu, W.; Scanlon, B.R.; Zhang, L.; Pan, M. Local and Global Factors Controlling Water-energy Balances within the Budyko Framework. *Geophys. Res. Lett.* **2013**, *40*, 6123–6129. [CrossRef]
42. Alonso Vicario, S.; Hornberger, G.M.; Mazzoleni, M.; Garcia, M. The Importance of Climate and Anthropogenic Influence in Precipitation Partitioning in the Contiguous United States. *J. Hydrol.* **2024**, *633*, 130984. [CrossRef]
43. Gentine, P.; D'Odorico, P.; Lintner, B.R.; Sivandran, G.; Salvucci, G. Interdependence of Climate, Soil, and Vegetation as Constrained by the Budyko Curve. *Geophys. Res. Lett.* **2012**, *39*, L19404. [CrossRef]
44. Nkiaka, E.; Okafor, G.C. Changes in Climate, Vegetation Cover and Vegetation Composition Affect Runoff Generation in the Gulf of Guinea Basin. *Hydrol. Process.* **2024**, *38*, e15124. [CrossRef]
45. Du, C.; Sun, F.; Yu, J.; Liu, X.; Chen, Y. New Interpretation of the Role of Water Balance in an Extended Budyko Hypothesis in Arid Regions. *Hydrol. Earth Syst. Sci.* **2016**, *20*, 393–409. [CrossRef]
46. Shao, Q.; Traylen, A.; Zhang, L. Nonparametric Method for Estimating the Effects of Climatic and Catchment Characteristics on Mean Annual Evapotranspiration. *Water Resour. Res.* **2012**, *48*, W03517. [CrossRef]
47. Yang, D.; Shao, W.; Yeh, P.J.-F.; Yang, H.; Kanae, S.; Oki, T. Impact of Vegetation Coverage on Regional Water Balance in the Nonhumid Regions of China. *Water Resour. Res.* **2009**, *45*, W00A14. [CrossRef]
48. Yang, D.; Sun, F.; Liu, Z.; Cong, Z.; Ni, G.; Lei, Z. Analyzing Spatial and Temporal Variability of Annual Water-Energy Balance in Nonhumid Regions of China Using the Budyko Hypothesis. *Water Resour. Res.* **2007**, *43*, W04426. [CrossRef]
49. Chen, Y.; Chen, X.; Xue, M.; Yang, C.; Zheng, W.; Cao, J.; Yan, W.; Yuan, W. Revisiting the Hydrological Basis of the Budyko Framework with the Principle of Hydrologically Similar Groups. *Hydrol. Earth Syst. Sci.* **2023**, *27*, 1929–1943. [CrossRef]
50. Ning, T.; Li, Z.; Liu, W. Vegetation Dynamics and Climate Seasonality Jointly Control the Interannual Catchment Water Balance in the Loess Plateau under the Budyko Framework. *Hydrol. Earth Syst. Sci.* **2017**, *21*, 1515–1526. [CrossRef]
51. Zhang, X.; Xiong, Z.; Yan, X. Modeling Precipitation Changes in the Heihe River Basin, Northwest China, from 1980 to 2014 with the Regional Integrated Environment Modeling System (RIEMS) Nested with ERA-Interim Reanalysis Data. *Theor. Appl. Clim.* **2019**, *137*, 493–503. [CrossRef]
52. Li, X.; Cheng, G.; Liu, S.; Xiao, Q.; Ma, M.; Jin, R.; Che, T.; Liu, Q.; Wang, W.; Qi, Y.; et al. Heihe Watershed Allied Telemetry Experimental Research (HiWATER): Scientific Objectives and Experimental Design. *Bull. Am. Meteorol. Soc.* **2013**, *94*, 1145–1160. [CrossRef]
53. Li, X.; Cheng, G.; Ge, Y.; Li, H.; Han, F.; Hu, X.; Tian, W.; Tian, Y.; Pan, X.; Nian, Y.; et al. Hydrological Cycle in the Heihe River Basin and Its Implication for Water Resource Management in Endorheic Basins. *J. Geophys. Res. Atmos.* **2018**, *123*, 890–914. [CrossRef]
54. Hu, G.; Jia, L. Monitoring of Evapotranspiration in a Semi-Arid Inland River Basin by Combining Microwave and Optical Remote Sensing Observations. *Remote Sens.* **2015**, *7*, 3056–3087. [CrossRef]
55. Zheng, C.; Jia, L.; Hu, G. Global Land Surface Evapotranspiration Monitoring by ETMonitor Model Driven by Multi-Source Satellite Earth Observations. *J. Hydrol.* **2022**, *613*, 128444. [CrossRef]
56. Zheng, C.; Jia, L. Global Canopy Rainfall Interception Loss Derived from Satellite Earth Observations. *Ecohydrology* **2020**, *13*, e2186. [CrossRef]
57. Allen, R.G.; Pereira, L.S.; Raes, D.; Smith, M. *Crop Evapotranspiration-Guidelines for Computing Crop Water Requirements-FAO Irrigation and Drainage Paper 56*; Food and Agriculture Organization: Rome, Italy, 1998; Volume 300, p. D05109.
58. Funk, C.C.; Peterson, P.J.; Landsfeld, M.F.; Pedreros, D.H.; Verdin, J.P.; Rowland, J.D.; Romero, B.E.; Husak, G.J.; Michaelsen, J.C.; Verdin, A.P. *A Quasi-Global Precipitation Time Series for Drought Monitoring*; U.S. Geological Survey Data Series: Reston, VA, USA, 2014; Series 832; p. 4.
59. Zhong, B.; Yang, A.; Nie, A.; Yao, Y.; Zhang, H.; Wu, S.; Liu, Q. Finer Resolution Land-Cover Mapping Using Multiple Classifiers and Multisource Remotely Sensed Data in the Heihe River Basin. *IEEE J. Sel. Top. Appl. Earth Obs. Remote Sens.* **2015**, *8*, 4973–4992. [CrossRef]
60. Zhong, B.; Yang, A.; Jue, K.; Wu, J. Long Time Series High-Quality and High-Consistency Land Cover Mapping Based on Machine Learning Method at Heihe River Basin. *Remote Sens.* **2021**, *13*, 1596. [CrossRef]
61. Simons, G.; Koster, R.; Droogers, P. *HiHydroSoil v2.0—A High Resolution Soil Map of Global Hydraulic Properties*; FutureWater report 134: Wageningen, The Netherlands, 2020.

62. Liu, S.; Li, X.; Xu, Z.; Che, T.; Xiao, Q.; Ma, M.; Liu, Q.; Jin, R.; Guo, J.; Wang, L.; et al. The Heihe Integrated Observatory Network: A Basin-Scale Land Surface Processes Observatory in China. *Vadose Zone J.* **2018**, *17*, 180072. [CrossRef]
63. Yan, X. *Estimation of Irrigation Efficience at Different Scales in the Middle Stream of Heihe River Irrigation District*; China Institute of Water Resources and Hydropower Research: Beijing, China, 2015.
64. Jiang, Y. *Simulation Analysis and Optimal Regulation for Agro-Hydrological Processes and Water Use Efficiency on Multiple Scales of the Middle Heihe River Basin*; China Agricultural University: Beijing, China, 2017.
65. Chen, X.; Sivapalan, M. Hydrological Basis of the Budyko Curve: Data-Guided Exploration of the Mediating Role of Soil Moisture. *Water Resour. Res.* **2020**, *56*, e2020WR028221. [CrossRef]
66. van Eekelen, M.W.; Bastiaanssen, W.G.M.; Jarmain, C.; Jackson, B.; Ferreira, F.; van der Zaag, P.; Saraiva Okello, A.; Bosch, J.; Dye, P.; Bastidas-Obando, E.; et al. A Novel Approach to Estimate Direct and Indirect Water Withdrawals from Satellite Measurements: A Case Study from the Incomati Basin. *Agric. Ecosyst. Environ.* **2015**, *200*, 126–142. [CrossRef]
67. Jia, L.; Shang, H.; Hu, G.; Menenti, M. Phenological Response of Vegetation to Upstream River Flow in the Heihe Rive Basin by Time Series Analysis of MODIS Data. *Hydrol. Earth Syst. Sci.* **2011**, *15*, 1047–1064. [CrossRef]
68. Dastane, N.G. *Effective Rainfall in Irrigated Agriculture*; FAO Irrigation and Drainage Paper No: 25; Food and Agriculture Organization: Rome, Italy, 1978.
69. Muratoglu, A.; Bilgen, G.K.; Angin, I.; Kodal, S. Performance Analyses of Effective Rainfall Estimation Methods for Accurate Quantification of Agricultural Water Footprint. *Water Res.* **2023**, *238*, 120011. [CrossRef]
70. Smith, M. (Ed.) *CROPWAT: A Computer Program for Irrigation Planning and Management*; FAO Irrigation and Drainage Paper No. 46; Food and Agriculture Organization: Rome, Italy, 1992; ISBN 978-92-5-103106-3.
71. Choudhury, B.J.; DiGirolamo, N.E. A Biophysical Process-Based Estimate of Global Land Surface Evaporation Using Satellite and Ancillary Data I. Model Description and Comparison with Observations. *J. Hydrol.* **1998**, *205*, 164–185. [CrossRef]
72. Schaake, J.C.; Koren, V.I.; Duan, Q.-Y.; Mitchell, K.; Chen, F. Simple Water Balance Model for Estimating Runoff at Different Spatial and Temporal Scales. *J. Geophys. Res. Atmos.* **1996**, *101*, 7461–7475. [CrossRef]
73. Li, X.; Cheng, G.; Fu, B.; Xia, J.; Zhang, L.; Yang, D.; Zheng, C.; Liu, S.; Li, X.; Song, C.; et al. Linking Critical Zone with Watershed Science: The Example of the Heihe River Basin. *Earth's Future* **2022**, *10*, e2022EF002966. [CrossRef]
74. Cai, W.; Jiang, X.; Sun, H.; Lei, Y.; Nie, T.; Li, L. Spatial Scale Effect of Irrigation Efficiency Paradox Based on Water Accounting Framework in Heihe River Basin, Northwest China. *Agric. Water Manag.* **2023**, *277*, 108118. [CrossRef]
75. Zhang, A.; Zheng, C.; Wang, S.; Yao, Y. Analysis of Streamflow Variations in the Heihe River Basin, Northwest China: Trends, Abrupt Changes, Driving Factors and Ecological Influences. *J. Hydrol. Reg. Stud.* **2015**, *3*, 106–124. [CrossRef]
76. Zhang, L.; Potter, N.; Hickel, K.; Zhang, Y.; Shao, Q. Water Balance Modeling over Variable Time Scales Based on the Budyko Framework—Model Development and Testing. *J. Hydrol.* **2008**, *360*, 117–131. [CrossRef]
77. Zang, C.; Liu, J.; Gerten, D.; Jiang, L. Influence of Human Activities and Climate Variability on Green and Blue Water Provision in the Heihe River Basin, NW China. *J. Water Clim. Chang.* **2015**, *6*, 800–815. [CrossRef]
78. Zhang, R.; Wang, L. Characteristics of Green and Blue Water Flow of Hydrological Landscapes of Upper Heihe in Northwest China. *J. Phys. Conf. Ser.* **2020**, *1637*, 012074. [CrossRef]
79. Hoogeveen, J.; Faurès, J.-M.; Peiser, L.; Burke, J.; van de Giesen, N. GlobWat—A Global Water Balance Model to Assess Water Use in Irrigated Agriculture. *Hydrol. Earth Syst. Sci.* **2015**, *19*, 3829–3844. [CrossRef]
80. Shang, K.; Yao, Y.; Di, Z.; Jia, K.; Zhang, X.; Fisher, J.B.; Chen, J.; Guo, X.; Yang, J.; Yu, R.; et al. Coupling Physical Constraints with Machine Learning for Satellite-Derived Evapotranspiration of the Tibetan Plateau. *Remote Sens. Environ.* **2023**, *289*, 113519. [CrossRef]
81. Zhao, W.L.; Gentine, P.; Reichstein, M.; Zhang, Y.; Zhou, S.; Wen, Y.; Lin, C.; Li, X.; Qiu, G.Y. Physics-Constrained Machine Learning of Evapotranspiration. *Geophys. Res. Lett.* **2019**, *46*, 14496–14507. [CrossRef]

Disclaimer/Publisher's Note: The statements, opinions and data contained in all publications are solely those of the individual author(s) and contributor(s) and not of MDPI and/or the editor(s). MDPI and/or the editor(s) disclaim responsibility for any injury to people or property resulting from any ideas, methods, instructions or products referred to in the content.